Prepared for submission to JINST

First results on new helium based eco-gas mixtures for the Extreme Energy Events Project

TO BE UPDATED, M. Abbrescia[a,b] C. Avanzini[c,d] L. Baldini[c,d] R. Baldini Ferroli[e] G. Batignani[c,d] M. Battaglieri[f] S. Boi[g,h] E. Bossini[d,1] F. Carnesecchi[i] F. Cavazza[j] C. Cicalò[h] L. Cifarelli[k,j] F. Coccetti[l] E. Coccia[m] A. Corvaglia[n] D. De Gruttola[o,p] S. De Pasquale[o,p] L. Galante[q] M. Garbini[l,j] G. Gemme[f] I. Gnesi[l,r] S. Grazzi[s,f] D. Hatzifotiadou[j,i] P. La Rocca[t,u] Z. Liu[v] G. Mandaglio[s,u] A. Margotti[j] G. Maron[w] M. N. Mazziotta[b] A. Mulliri[g,h] R. Nania[j] F. Noferini[j] F. Nozzoli[x] F. Palmonari[k,j] M. Panareo[y,n] M. P. Panetta[n] R. Paoletti[z,d] C. Pellegrino[aa] L. Perasso[f] O. Pinazza[j] C. Pinto[ab] S. Pisano[l,e] F. Riggi[t,u] G. Righini[ac] C. Ripoli[o,p] M. Rizzi[b] G. Sartorelli[k,j] E. Scapparone[j] M. Schioppa[ad,r] G. Scioli[k,j] A. Scribano[z,d] M. Selvi[j] M. Taiuti[ae,f] G. Terreni[d] A. Trifirò[s,u] M. Trimarchi[s,u] C. Vistoli[aa] L. Votano[i32] M. C. S. Williams[i,v] A. Zichichi[l,k,j,i,v] R. Zuyeuski[v,i]

[a]*Dipartimento di Fisica dell'Università e del Politecnico di Bari, Via Amendola 173, 70125 Bari, Italy*

[b]*INFN, Sezione di Bari, Via Orabona 4, 70126 Bari, Italy*

[c]*Dipartimento di Fisica, Università di Pisa, Largo Bruno Pontecorvo 3, 56127 Pisa, Italy*

[d]*INFN, Sezione di Pisa, Largo Bruno Pontecorvo 3, 56127 Pisa, Italy*

[e]*INFN, Laboratori Nazionali di Frascati, Via Enrico Fermi 54, 00044 Frascati, Italy*

[f]*INFN, Sezione di Genova, Via Dodecaneso, 33, 16146 Genova, Italy*

[g]*Dipartimento di Fisica, Università di Cagliari, S.P. Monserrato-Sestu, Monserrato (CA), 09042, Italy*

[h]*INFN, Sezione di Cagliari, Complesso Universitario di Monserrato, S.P. per Sestu, 09042, Monserrato (CA), Italy*

[i]*CERN, Esplanade des Particules 1, 1211 Geneva 23, Switzerland*

[j]*INFN, Sezione di Bologna, Viale Carlo Berti Pichat 6/2, 40127 Bologna, Italy*

[k]*Dipartimento di Fisica e Astronomia, Università di Bologna, Viale Carlo Berti Pichat 6/2, 40127 Bologna, Italy*

[l]*Museo Storico della Fisica e Centro Studi e Ricerche "E. Fermi", Via Panisperna 89/a, 00184 Roma, Italy*

[1]Corresponding author.

[m]*Gran Sasso Science Institute,*
Viale Francesco Crispi 7, 67100 L'Aquila, Italy
[n]*INFN, Sezione di Lecce,*
Via per Arnesano. 73100, Lecce, Italy
[o]*Dipartimento di Fisica, Università di Salerno,*
Via Giovanni Paolo II, 132, 84084 Fisciano SA, Italy
[p]*INFN ,Gruppo Collegato di Salerno,*
Complesso Universitario di Monte S. Angelo ed. 6 via Cintia, 80126, Napoli, Italy
[q]*Teaching and Language Lab, Politecnico di Torino,*
Corso Duca degli Abruzzi 24, Torino, Italy
[r]*INFN, Gruppo Collegato di Cosenza,*
via Pietro Bucci, Rende (Cosenza), Italy
[s]*Dipartimento di Scienze Matematiche e Informatiche, Scienze Fisiche e Scienze della Terra, Università di Messina,*
Viale Ferdinando Stagno d'Alcontres 31, 98166 Messina (ME), Italy
[t]*Dipartimento di Fisica, Università degli Studi di Catania,*
Via. S. Sofia 64, 95123 Catania (CT), Italy
[u]*INFN, Sezione di Catania,*
Via. S. Sofia 64, 95123 Catania (CT), Italy
[v]*ICSC World laboratory,*
Geneva, Switzerland
[w]*INFN, Laboratori Nazionali di Legnaro,*
Viale dell'Università 2, 35020 Legnaro, Italy
[x]*INFN Trento Institute for Fundamental Physics and Applications,*
Via Sommarive, 14, 38123 Povo TN, Italy
[y]*Dipartimento di Matematica e Fisica, Università del Salento,*
Via per Arnesano. 73100, Lecce, Italy
[z]*Dipartimento di Scienze Fisiche, della Terra e dell'Ambiente, Università di Siena,*
Via Roma 56 - 53100 Siena
[aa]*INFN-CNAF,*
Viale Carlo Berti Pichat 6/2, 40127 Bologna
[ab]*Physik Department, Technische Universitat Munchen,*
James-Franck-Straße 1, 85748 Garching bei München
[ac]*CNR, Istituto di Fisica Applicata "Nello Carrara",*
Via Madonna del Piano 10, 50019 Sesto Fiorentino (FI), Italy
[ad]*Dipartimento di Fisica, Università della Calabria,*
via Pietro Bucci, Rende (Cosenza), Italy
[ae]*Dipartimento di Fisica, Università di Genova,*
Via Dodecaneso, 33, 16146 Genova GE
[af]*INFN, Laboratori Nazionali del Gran Sasso,*
Via G. Acitelli 22, 67100 Assergi (AQ), Italy

E-mail: edoardo.bossini@pi.infn.it

Abstract: The Extreme Energy Events (EEE) experiment, a joint project of the Centro Fermi and INFN Italian national research institutes, has a dual purpose: a scientific research program on cosmic rays at ground level and an intense outreach and educational program. The project counts about 60 tracking detectors mostly hosted in Italian high schools, each made by three Multigap Resistive Plate Chambers, operated so far with a gas mixture composed by 98% $C_2H_2F_4$ and 2% SF_6. Due to its high Global Warming Potential, a few years ago the EEE collaboration has started an extensive R&D on alternative mixtures environmentally sustainable and compatible with the current experimental setup and operational environment. Among others gas mixtures, the one with helium and hydrofluoroolefine R1234ze gave the best result during the preliminary test performed in two of the network telescopes. The detector has proved to reach performance levels comparable to those obtained with previous mixtures, without any modification of the hardware. We will discuss the first results obtained with the new mixture, tested with different percentages of the two components.

Keywords: Multigap Resistive-plate chambers; Cosmic-ray telescope; Eco-mixtures for gas detectors

Contents

1 Introduction

The Extreme Energy Events (EEE) experiment[1] is based on a network of about 60 cosmic-ray measuring stations (called telescopes) installed mostly in High Schools all over Italy (Fig. 1). The students of the schools involved in the project have the unique opportunity to participate in

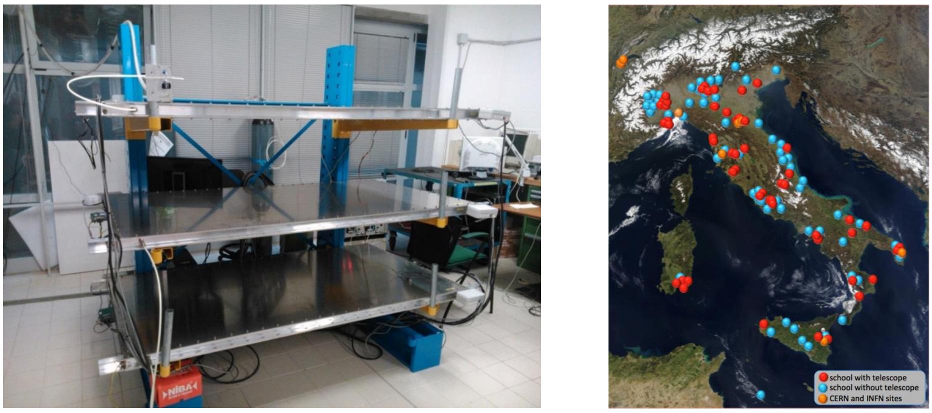

Figure 1: On the left, a picture of one of the EEE telescopes. On the right, the geographical distribution of the schools participating to the project with (red dots) or without a telescope (blu dots). Some telescopes are installed in INFN sites or at CERN (orange dots). THE RIGHT ONE NEEDS AN UPDATE

the construction of the detectors at CERN, in the installation inside their own schools and in the commissioning, operations and monitoring of the telescope all over the yearly data taking periods. Telescope data are centrally collected at the INFN-CNAF data center in Bologna, were the Data Quality Monitoring and data analysis are automatically performed.
Each telescope is able to detect and track the traversing particles with multi-tracking capability and

assign a precise absolute timestamp to each particle using the Global Positioning System (GPS). Cosmic rays detected by individual telescopes can be thus correlated (offline) and data analyses on extensive air showers are possible. The performance of the detectors[2] and the wide geographical distribution of the telescopes allow for a broad research program on cosmic rays at ground level. The telescopes are made of 3 Multigap Resistive Plate Chambers (MRPC) separated by about 50 cm, as shown in Fig. 1. The active volume is divided is 6 gaps separated by 1.1 mm thick glasses (see Fig. 2), with a total active surface of 158x82 cm^2 [3]. Two sets of telescopes have been produced, one with 300 μm gaps and the other with 250 μm gaps. The bias voltage is applied on the external sides of the two outer glasses, painted with a resistive paint. The induced signals are read out by 24 longitudinal strip pairs, located on the the top and bottom part of the chamber with a pitch of 3.2 cm (see Fig.2). Each of the top strips is aligned and paired with a bottom strip, providing a differential readout scheme and is therefore treated as a single readout strip in the rest of the article.

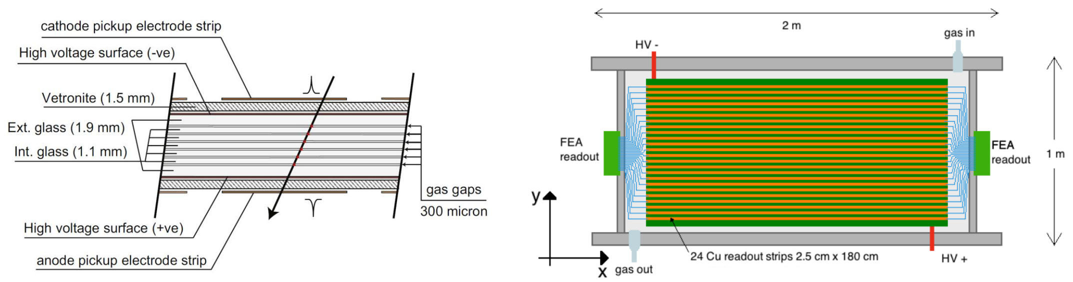

Figure 2: On the left, a schematic representation of a six gap MRPC stack. On the right, the schematic top view of one MRPC with the 24 top strips read out by the two front-end boards. The top strips are paired with the bottom strips, providing a differential readout scheme, and each pair is treated as a single readout channel.

Whenever a signal is generated in the detector, the signal travels to both ends of the strips, where it is discriminated and digitized by the NINO chips[4], which are fast 8-channel discriminators designed with a full differential architecture, located on the front-end boards. The digitized output of the NINO chips follows the Low-Voltage Differential Signaling (LVDS) standard, with an output signal duration, here referred as Time Over Threshold (TOT), which depends from the total input charge. The NINO is followed by a Time to Digital Converter (the CERN HPTDC[5]), able to measure the time of arrival of both the leading and trailing edges of the input signals. It is therefore possible to acquire a precise timestamp for the time of arrival of the signal, together with the measurement of the TOT. The reconstruction algorithm, as described in Sec. 3, can then use the time information from both strip ends to reconstruct a 2-dimensional hit on the chamber, and assign the timestamp to it. Precise timing is crucial to measure some of the particle characteristics (i.e. the speed and time of flight between the top-bottom chambers) and for a precise reconstruction of hit coordinates. The main source of uncertainty when measuring of the time of arrival in the EEE MRPCs is generated by the Time Walk (TW) of the signal, originating from the fluctuation of the

charge released and amplified in the detector. However, the TOT information can be used offline to correct for the signal TW, enhancing the time precision of the apparatus.
After clusterization, the hits on the three chambers are then used to reconstruct the particle track. The absolute particle timestamp is finally computed merging the particle timestamp with the synchronization signal provided by the GPS. The uncertainty on the absolute particle timestamp is usually dominated by the precision of the time precision of the GPS, of the order of few tens of ns.

2 New eco-mixtures

Until the end of 2021 the MRPCSs have been fluxed with a gas mixture 98% $C_2H_2F_4$ (R134a) and 2% SF_6, both GreenHouse Gases(GHG), with total Global Warming Potential (GWP) ~1880. In order to reduce operational costs of the telescopes and the emissions of GHGs, a dedicated campaign, started in 2019 and terminated after the stop for the COVID-19 pandemic, allowed to reduce the gas flux to ~1 l/h (from the previous 2-3 l/h) for the large majority of the telescopes. Despite such improvement, the search for new eco-friendly gas mixtures has become crucial for the EEE project, especially given its important role in outreach and student education. Therefore the EEE collaboration has decided to phase out the gas mixture in use and start an R&D on alternative mixtures environmentally sustainable. Several physics experiment all over the world are pursuing the same strategy, making the search for new eco-friendly mixtures one of the most relevant topics in the field of gaseous detector development. In the R&D some strict requirements are posed on the typology and performance of the new gas mixture, deriving from budget constraints and from the security regulation in force in the schools were the telescopes are located:

- only non flammable, non toxic gases are allowed;
- to match the requirements of the existing mixers, only binary mixtures can be used;
- the detector must able to operate with a maximum bias voltage of 20 kV;
- the front-end electronics must be able to handle the new signals;
- the new detector performance should not have any negative impact on the physics program of the experiment;
- the cost of the mixture should be in line with the old one.

Among all the constraints, the most limiting are represented by the restriction to binary mixtures and the upper limit on the bias voltage. Several results are indeed available on new eco-mixtures for RPC detectors, but all of them make use of three or more gases. The strategy adopted was to replace the R134a with the HydroFluoroOlefine (HFO) R1234ze ($C_3H_2F_4$), the most similar molecule with low GWP=4 and compliant with the security requirements, and add an almost equal percentage of helium or CO_2 to the mixture, with the effect of reducing the operating voltage within the allowed range. A pure HFO1234ze is indeed expected to require a higher bias voltage, higher than the one which can be currently generated. It is wort noticing that with both CO_2 and He, the total GWP remains below 10. The expected drawback of the strategy is represented by a reduced quenching capacity of the new compounds with respect to the standard mixture with SF_6. Both

CO_2 and He based compounds have been extensively tested in the EEE collaboration. In particular, the mixture made of HFO1234ze (simply HFO in the rest of the text) and helium has been tested on the telescope located in the Rende (codename REND-01) site, hosted in an INFN laboratory, providing the best results to date.

3 Test setup

The results of the R&D program reported here have been obtained testing the middle chamber fluxed with the HFO+He mixture, while operating the 2 outer chambers of the telescope with the "standard" (R134a+SF6) mixture.
The external chambers are used as reference for trigger and tracking. The data, collected by triggering on the coincidence of these reference chambers, have been analyzed offline with a dedicated algorithm. As previously discussed, chamber signald are digitized at both ends of the strips, generating End Hits (EH). An EH contains the leading edge time and the TOT of the signal. The first step of the reconstruction is the pairing of EHs. The HPTDC is set to acquire all EHs within a time match window of 500 ns, set with a proper latency w.r.t. the trigger arrival time. The matching window is further reduced in the offline reconstruction to ~100 ns. EHs are ordered in time and for each strip end only the first EH found in the offline match window is retained. If a strip has EHs on both ends, a hit on the chamber is formed. While the Y coordinate is directly extrapolated from the identifying strip number, the longitudinal coordinate X is computed from the difference of the times of arrival of the 2 EHs, providing a 2-dimensional hit position. The average of the two arrival times, insensitive to the hit postion, is in turn used to assign a precise timestamp to the hit, providing a 4D measurement (Z being fixed by the vertical position of the chamber).
Next, the clusterization is performed through an iterative procedure. First a hit list is formed. The first hit is promoted to cluster and removed from the hit list, then the algorithm searches for another hit closer than 10 cm to the cluster. If found, it is added to the cluster and removed from the list. The search starts back from the first hit still in the list and goes ahead till the list is empty or no hit matching the cluster is found. In case the list contains other hits, the procedure starts again, creating a new cluster. It is important to note that the distance between a cluster and a hit is the minimum distance between the hit and all the hits already assigned to the cluster. Finally, the cluster coordinate is computed as the average of all hits coordinates. In the present analysis the information of the TOT has not been used to correct the hit timestamps. The timestamp of a cluster has been defined as the timestamp of the hit with the lowest time of arrival. This definition allows to achieve better performance compared to the average of all hit timestamps. Work is ongoing to establish the best TW correction algorithm or to perform a weighted average of all time measurements in the cluster, with weights derived from the TOTs of the hits. The track reconstruction algorithm, after the hit clusterization, checks if exactly one cluster is present in both triggering chambers, in practice selecting events with a single track to avoid ambiguities in the reconstruction. If the condition is met, it generates a candidate track using the clusters from the two reference chambers. The candidate track is then projected (in both space and time) in the chamber under test. To reduce the background, dominated by spurious coincidences and upgoing particles, the following selection criteria are applied for the candidate tracks to be used in the final computation of the efficiency:

- a particle speed β in the range $0.75 < \beta < 1.25$ (within errors);

- a track projection on the chamber under test within a fiducial area, defined with a clearance of 15 cm from the edge of the active surface.

Events with tracks passing the selection criteria are then used to check the efficiency of the chamber under test. The chamber under test is considered efficient if a cluster is found within 15 cm and 10 ns from the extrapolated track hit. If more than one cluster is matching such condition, the closest in space is retained for the computation of the time-space residuals.

On top of the efficiency other parameters are computed as a function of the bias voltage, among which:

- the streamer fraction, defined as the fraction of efficient events with a matching cluster in the test chamber made by more then 3 hits. Clusters defined as streamer are not excluded in the analysis;
- the average cluster size, defined as the average number of hits forming the matching cluster (even if defined as streamer);
- the time residual, defined as the time difference between the matching cluster time and the extrapolated track hit time;
- the spatial residuals, defined as the differences between the coordinates of the matching cluster center and the extrapolated impact point of the track.

The results reported in the next section have been obtained with with different HFO and He relative percentages (50/50,60/40,70/30 and pure HFO) and compared with the "standard" mixture. Gas flow has been kept around 1 l/h. For each mixture a High Voltage (HV) scan on the chamber under test has been performed, keeping the other two chambers at a fixed HV. As anticipated in Sec. 2, mixtures with large fractions of HFO are expected to have a significant increase in the operating voltage, above 20 kV. To produce such a bias voltage, above the actual reach of the existing power supply units of the EEE telescopes, a different high voltage system from CAEN[6] has been used for the tests reported herein. The system was able to deliver up to 24 kV differential bias voltage to the chambers.

4 Results

In Fig. 3a the efficiency of the chamber as a function of the effective bias voltage HV_{eff} using different gas mixtures is reported. The effective bias voltage is compensated for temperature and pressure effect, according to the formula $HV_{eff} = HV * \frac{P_{ref}}{P} * \frac{T}{T_{ref}}$, where $P_{ref} = 1010$ mbar and $T_{ref} = 20°$C. The data show, as expected, a reduction of the HV working point as the percentage of helium increases. A mixture 60/40 of HFO and helium respectively, provides very similar results in terms of efficiency with respect to the standard mixture. An efficiency plateau above 90% can be reached with a bias voltage below the 20 kV upper limit of the current experimental setup, using a mixture with at least 40% of helium. The uniformity of the chamber efficiency in the fiducial area can be seen in the plot of Fig. 3b, for the 50/50 mixture and an effective bias voltage of ~ 18 kV. The X-Y position is the one extrapolated on the test chamber using the two external reference

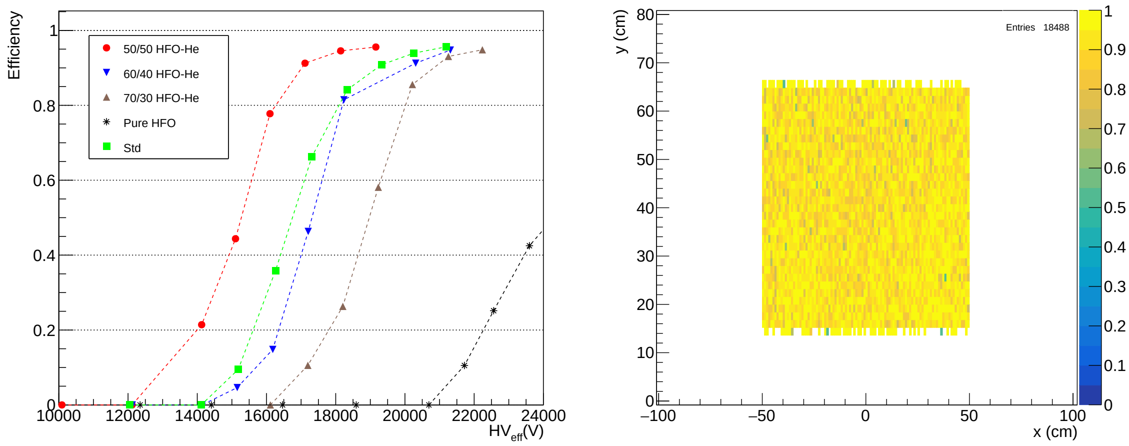

(a) Efficiency scan

(b) Efficiency map

Figure 3: On the left, the scan of efficiency for the chamber under test with different mixtures as a function of the applied effective bias voltage. On the right, the efficiency map for the 50/50 HFO-He mixture and an effective bias voltage of $\sim$ 18 kV in the fiducial area.

chambers.

As discussed in Sec. 2 the absence of a quencher is expected to have a negative impact on the streamer probability and on the cluster size. The results reported in Fig. 4 confirm this hypothesis. Both cluster size and streamer probability increase faster with the bias voltage than when using the standard mixture (4a and 4c). An efficiency above 90% can still be reached with a cluster size below $\approx$ 3 and a streamer fraction $\sim$ 0.1 (Fig. 4b and 4d respectively). While the cluster size can be easily handled by the offline clustering algorithm, the streamer fraction could pose some challenges in the reconstruction of the events, as well as for the potential aging effect on the detector. Mixtures with percentages of helium above 50% have not been tested, since the streamer probability and cluster size are expected to exceed the allowed operation limits, and since the desired operating voltage range was already obtained.

Spatial residuals have been computed independently for the two coordinates. Residuals in the Y direction are not expected to change, being dominated by the strip quantization and expected to be $\approx$ 1 cm. This is indeed confirmed for all mixtures and voltages, except for the 50/50 mixture at higher voltage. In that condition the percentage of streamers gets above 30% and the degradation in performance is due to a non optimal treatment of very large clusters, that is currently being addressed. Residuals in the X direction, computed using the time information as previously described, are instead a relevant parameter for the detector. The distribution of residual for three HFO-He mixtures and for the standard mixture are reported in Fig. 5. The voltages were selected in order to obtain an efficiency of 95%. The double gaussian fit is the same used in some previous EEE study, as reported elsewhere [2] and can successfully describe both standard and new mixtures. The standard deviation of the narrower gaussian is in the range 1.4-1.6 cm for all mixtures, no significant

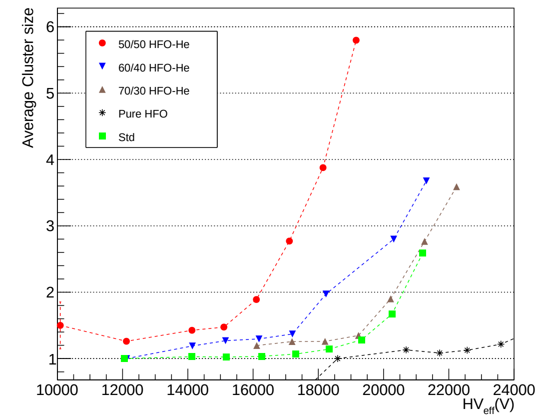

(a) Cluster size Vs HV

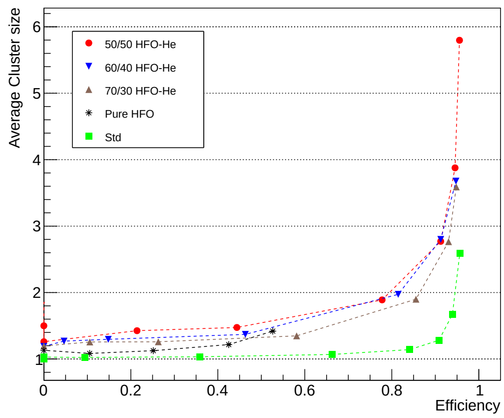

(b) Cluster size Vs Efficiency

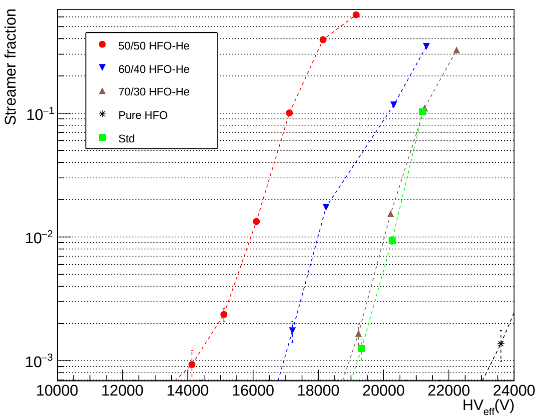

(c) Streamer Vs HV

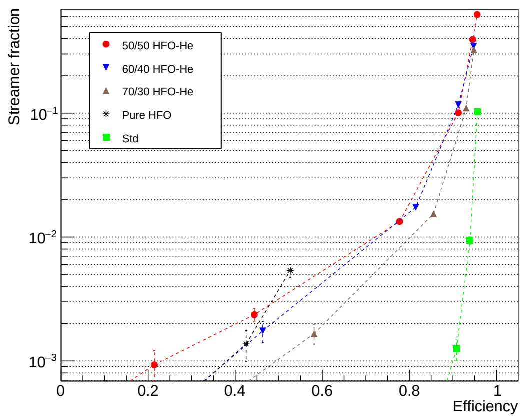

(d) Streamer Vs Efficiency

Figure 4: Cluster size (top) and streamer fraction (bottom), as a function of the HV (left) and efficiency (right).

differences are found. This could be expected as any difference in the signal shape and charge among different mixtures alters the signal detection time, but it cancels out being the X coordinate the difference of the arrival time of the same signal at the the two strip ends, hence automatically removing any TW effect. Secondary effects are within the uncertainties of the detector.

Residuals have been computed, for the same data, also for the cluster time. For all mixtures a strip-by-strip time calibration has been applied. This is indeed needed to correct for possible time offsets generated by the setup (i.e. different lengths of cables or fixed offsets in TDC channels). Since such offsets are not gas dependent, the correction has been computed only once using the standard mixture and then applied to all measurements. The resulting distributions are shown in Fig. 6. Differently from the standard mixture, the distributions with HFO-He mixtures show a pronounced tail on the left side of the peak. Gaussian fits have been performed excluding the tails,

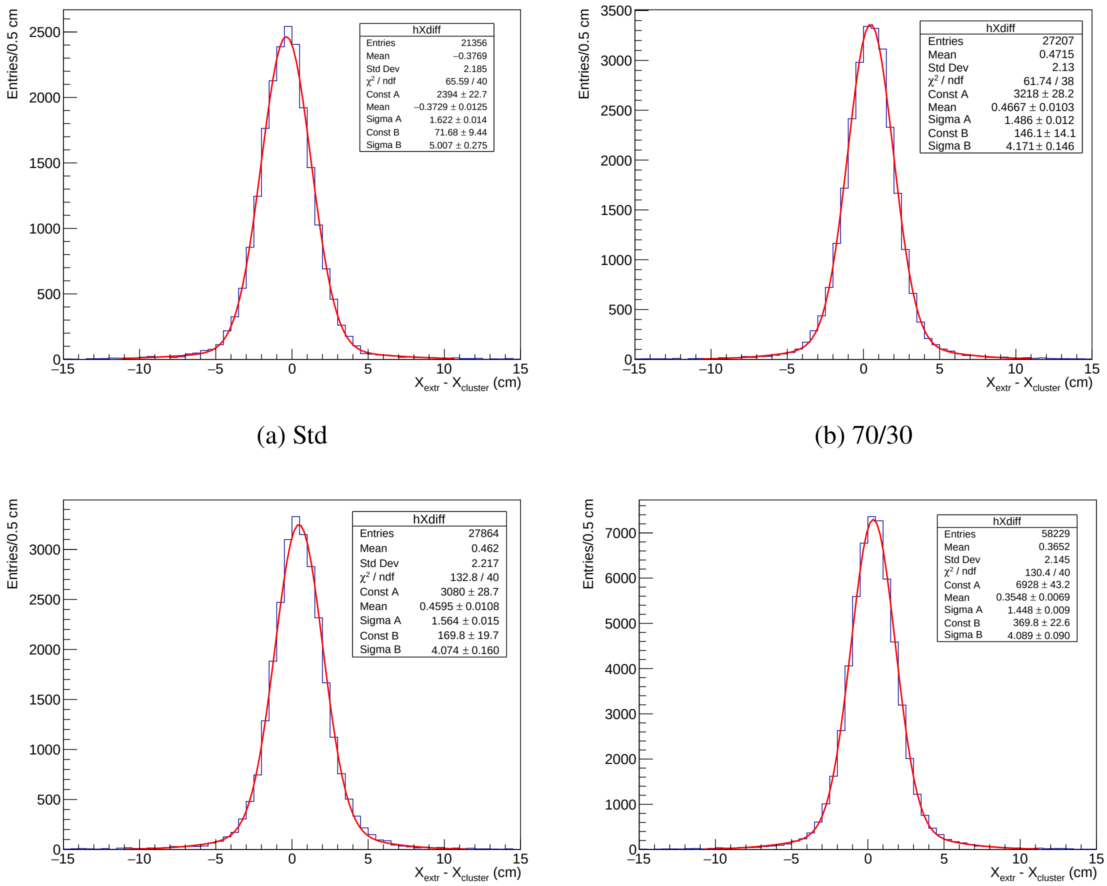

(a) Std

(b) 70/30

(c) 60/40

(d) 50/50

Figure 5: Distribution of the spatial residuals in the longitudinal X coordinate for the chamber under test, using the standard mixture and 3 HFO-He mixtures

corresponding to a fraction of outliers in the range 8-9%. The time residuals show a slight increase with respect to the standard mixture, suggesting a slightly lower time precision of the detector with the new mixture. The lower time precision can be interpreted, taking into account the above mentioned results on the cluster size and streamer fraction, as an effect due to the generation of larger signals in the chamber, not well tuned with the current front-end electronics. This can cause saturation and consequent loss of time precision. Further studies and offline calibrations based on TW corrections, not applied in the present analysis, can improve the detector performance, likely reducing the tails. No impact is also expected on the absolute particle timestamp since, as discussed in Sec. 1, its uncertainty is dominated by the GPS precision. The only parameter affected will the the particle time of flight and consequently, the measurement of its speed. The results shows that the efficiency, the tracking performance and the capability to correlate tracks detected by different telescopes of the network are unaltered by the new mixtures, preserving the physics program of the experiment.

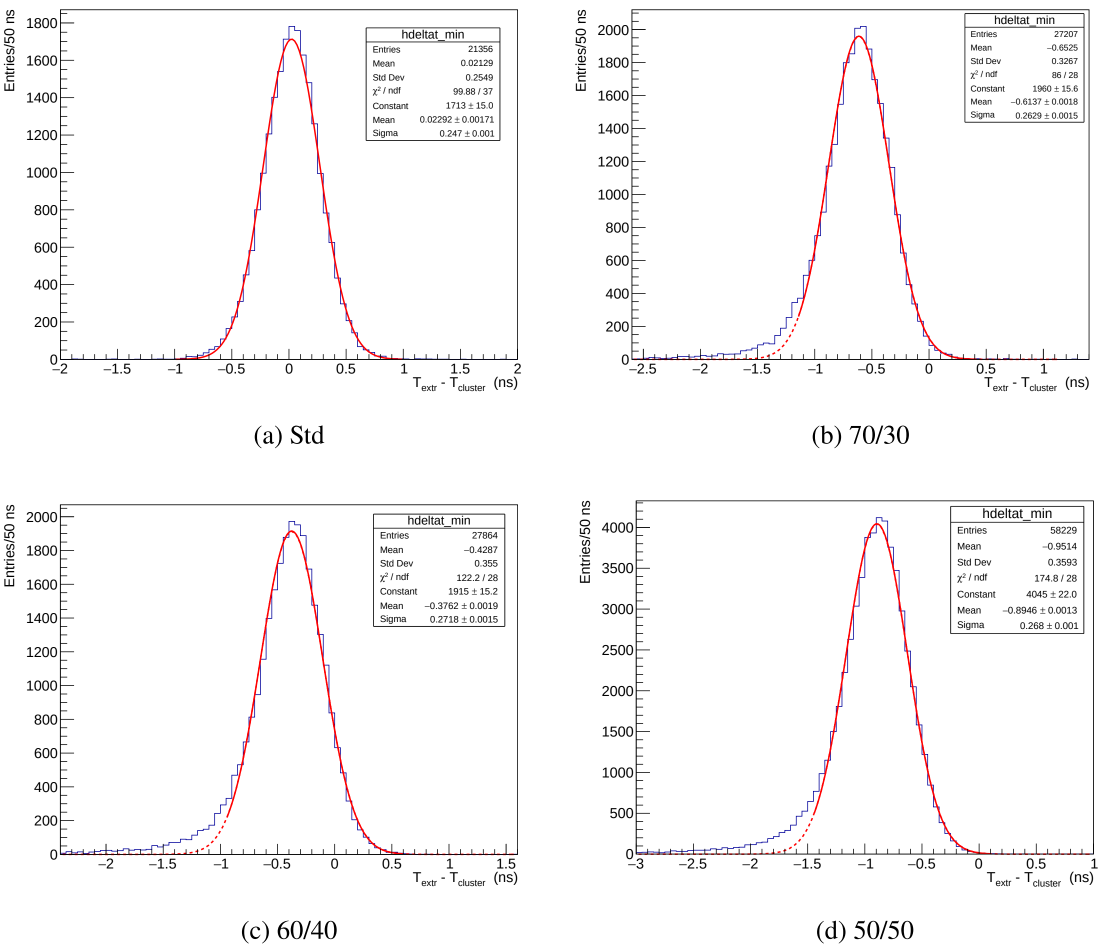

(a) Std (b) 70/30

(c) 60/40 (d) 50/50

Figure 6: Distribution of the time residuals for the chamber under test, using the standard mixture and three different HFO-He mixtures. The dashed lines represent the extrapolation of the fits to the tail regions.

5 Conclusions and outlook

TO BE DONE ACCORDINGLY TO FINALIZED RESULTS

6 Internal reference - THIS SECTION IS FOR INTERNAL USE ONLY

References

[1] A.Zichichi, *PROGETTO "LA SCIENZA NELLE SCUOLE " EEE – EXTREME ENERGY EVENTS* (Sep, 2017).

[2] EEE collaboration, *The Extreme Energy Events experiment: an overview of the telescopes performance*, *JINST* **13** (2018) P08026 [1805.04177].

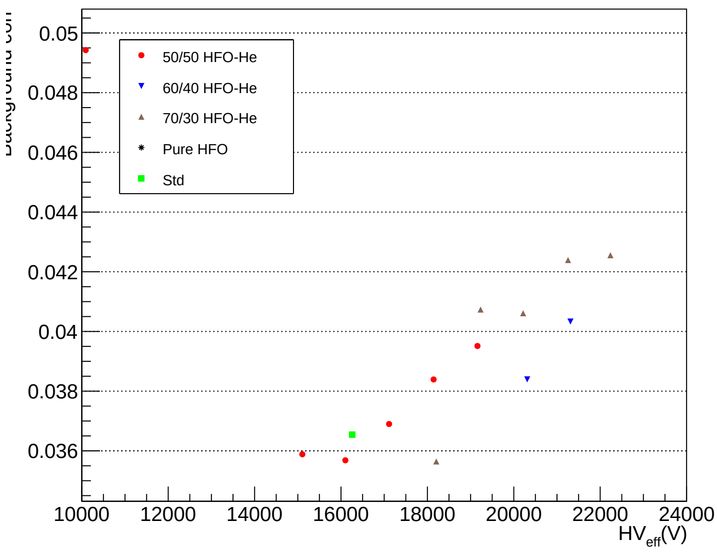

Figure 7: EEE INTERNAL USE ONLY : draft plot of relative percentage of residual background correction applied to efficiency.

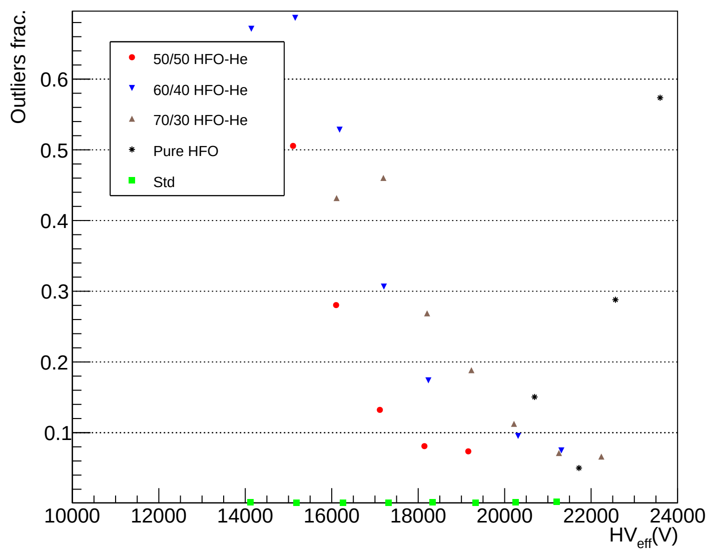

Figure 8: EEE INTERNAL USE ONLY : Draft plot of the number of outliers excluded from the Tresidual fit

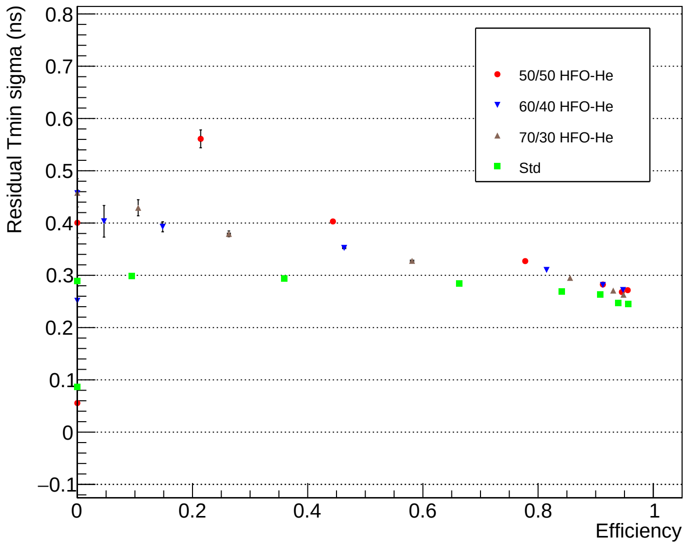

Figure 9: EEE INTERNAL USE ONLY : draft plot of timing residuals Vs efficiency.

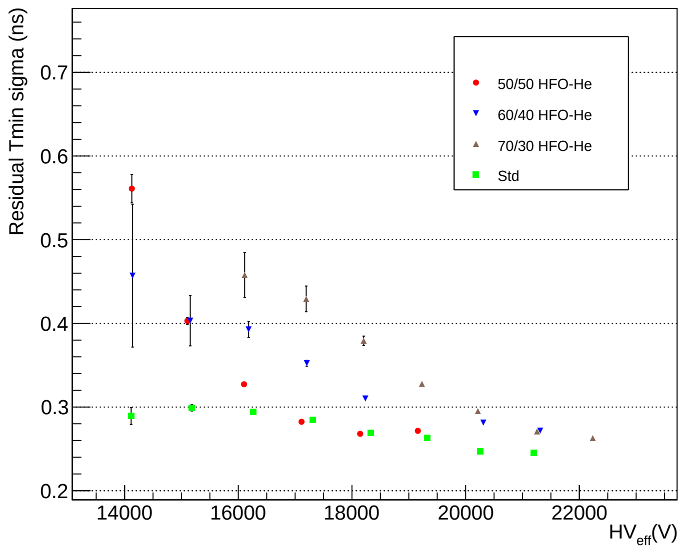

Figure 10: EEE INTERNAL USE ONLY : draft plot of timing residuals Vs HV.

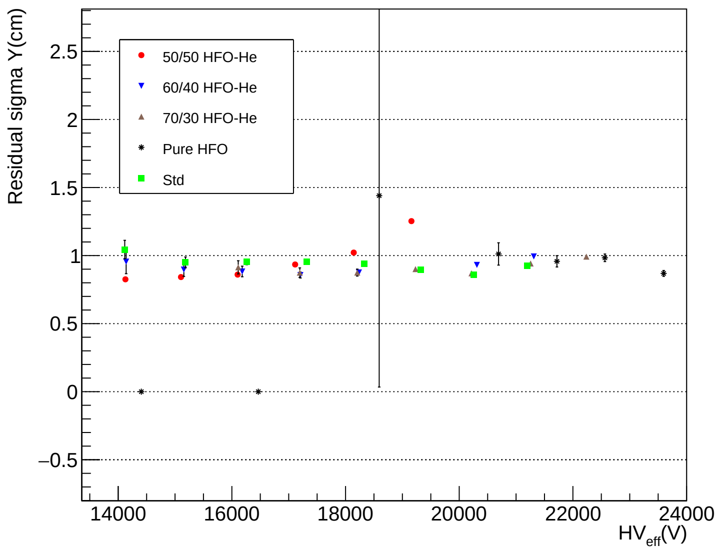

Figure 11: EEE INTERNAL USE ONLY :draft plot of Y residuals (fit sigma) Vs HV (quite miningless due to strip quantization).

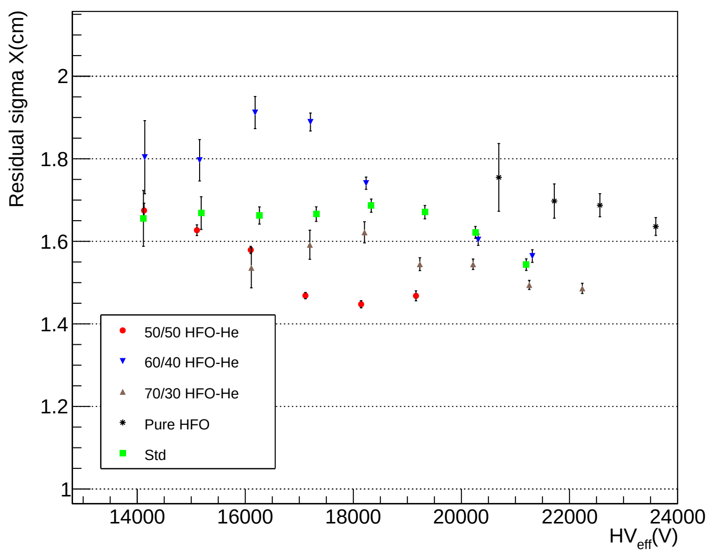

Figure 12: EEE INTERNAL USE ONLY :draft plot of X residuals (main gaussian sigma) Vs HV .

[3] M. Abbrescia et al., *Performance of a six gap MRPC built for large area coverage*, *Nucl. Instrum. Meth. A* **593** (2008) 263.

[4] F. Anghinolfi et al., *NINO: An ultra-fast and low-power front-end amplifier/discriminator ASIC designed for the multigap resistive plate chamber*, *Nucl. Instrum. Meth. A* **533** (2004) 183.

[5] J. Christiansen, *HPTDC High Performance Time to Digital Converter*, Geneva (2004).

[6] CAEN, "CAEN A7512DB." `https://www.caen.it/products/a7512db/` [Accessed: (20/06/2024)].